Investigation of Thermal Effects on Nailed Connection of Mass Ply Panels

Tu X. Ho
Detlef C. Laughery
Arijit Sinha

Abstract

Mass ply panels (MPP), a relatively new mass timber product, has been utilized in several construction projects as diaphragm and wall panels. Connection for MPP is a crucial structural component that requires a better understanding. This article presents an experimental investigation into elevated temperature exposure–driven property degradation of MPP nailed connections, which is important for both the design of new structures in terms of fire resistance and the rehabilitation of structures partially damaged by fire. One control group and 32 exposure groups, which were combinations of eight elevated temperatures and four exposure durations, were investigated. The failure modes and yield strength of the nailed connection were analyzed as a function of elevated temperature and exposure time and compared with the prediction from the National Design Specification and existing literature. The results show a decrease of up to 45 percent in initial stiffness and ultimate load; meanwhile, there was no statistical evidence for the change in yield load in the majority of testing groups. Two analytical models, namely, multilinear regression and first-order kinetics model, were proposed to model the degradation of initial stiffness and ultimate strength. The kinetics model provided a better prediction and suggested that the initial stiffness and ultimate strength of the nail connection degraded over time at rates depending on the exposure temperature.

An increasing interest in renewable and sustainable materials and recent advances in engineered wood products have driven the applications of mass timber in mid-rise to tall buildings. Mass ply panel (MPP) is a relatively new mass timber product and is gaining rapid acceptance in the construction industry. MPP is produced by Freres Engineered Wood, a premier wood products manufacturing company based in Oregon, USA. MPP is made by 25.4-mm-thick laminated veneer lumber (LVL) panels stacked together and glued with a structural-grade adhesive. A typical MPP consists of two face panels and several core panels based on the desired thickness. Each LVL panel is constructed with 1.6E-rated Douglas-fir veneer layers, of which seven layers are aligned in the long-ply direction and two layers in the cross-ply direction. MPP can be manufactured with different dimensions up to 3.66 m wide by 14.60 m long and a maximum thickness of 304.8 mm for roof, floor, and wall panel applications and 609.6 mm for beam and column applications.

MPP is a relatively new product, so there have been limited studies on mechanical properties and structural connection performance (Miyamoto et al. 2020; Morrell et al. 2020; Soti et al. 2020, 2021; Dillard et al. 2021; and Ho et al. 2022). One of the knowledge gaps is the performance of MPP connections under exposure to elevated temperatures (thermal effect), which is important for both the design of new structures in terms of fire resistance and the rehabilitation of structures partially damaged by fire. This study presents an experimental investigation on strength and stiffness degradation of nailed connections of MPP after exposure to elevated temperatures. The test results were compared with a prediction based on the results of a previous study reporting dowel bearing strength degradation (Dillard et al. 2021). Moreover, two analytical models were developed to predict the MPP connection's strength and stiffness degradation.

Literature Review

Studies on the mechanical performance of wood connections have been conducted primarily at ambient temperatures, and therefore limited data exist on the behavior of connections after exposure to elevated temperatures.

The authors are, respectively, PhD and Postdoctoral Scholar (tu.ho@oregonstate.edu [corresponding author]); Undergraduate Student (laugherd@oregonstate.edu); and Professor and Jeld-Wen Chair, Dept. of Wood Sci. and Engineering, Oregon State Univ., Corvallis (arijit.sinha@oregonstate.edu). This paper was received for publication in June 2022. Article no. 22-00039.

Forest Prod. J. 72(4):241–252.
doi:10.13073/FPJ-D-22-00039

Exposure to elevated temperatures causes an irreversible change in the mechanical properties of wood and wood connections (Fuller 1990; Shrestha et al. 1995; Noren 1996; Peyer and Cramer 1999; Sinha et al. 2011a, 2018; Akgul and Sinha 2016). Sinha et al. (2018) comprehensively reviewed studies on the degradation of wood connections after exposure to elevated temperatures. Strength degradation has been modeled generally in two ways: statistical and analytical. Statistical modeling is based on multiple linear regression (MLR), while analytical modeling tries to discern the underlying causes using first-order kinetics. These predictive models were used for thermal degradation of bending properties in wood composites (Sinha et al. 2011b, 2011c, 2012; Sinha 2013) and then expanded to thermal degradation of wood-sheathing nailed connection (Akgul and Sinha 2016; Sinha et al. 2018), bracket connection of cross-laminated timber (Mahr et al. 2020), and dowel bearing strength of MPP (Dillard et al. 2021). Both models showed good predictive results for thermal degradation. However, the kinetics-based model was preferable because of its better prediction capabilities and for using one less parameter than the regression-based model.

In recognition of the thermal effects on strength of wood materials and wood connection, the National Design Specification (NDS) (American National Standards Institute/American Wood Council [ANSI/AWC] 2015) introduced a temperature factor (C_t) that is used to decrease the design value when the connection is subjected up to 150°F for a sustained period of time. The maximum reduction in the design value is 30 percent for connections in dry conditions. NDS also includes provisions for the fire design of wood members. It is important to note that there are two main goals for fire-resistant design. The first objective is to support structural integrity during the fire and to allow inhabitants time to fully evacuate. The second is to remodel and modernize structures partially damaged by fire. Thus, it is extremely important to know the strength of the materials and connections so that performance simulations can be carried out and rehabilitation plans can be designed (Akgul and Sinha 2016). Since MPP is a relatively new mass timber material, Dillard et al. (2021) is the only study that was found on the effects of elevated temperature on MPP performance. A total of 198 specimens were fabricated for the dowel bearing test. There was one control group at ambient temperature of 25°C and 32 exposure groups, which are combinations of four different time exposures (0.5, 1, 1.5, and 2 h) and eight elevated temperatures (75°C, 100°C, 120°C, 140°C, 160°C, 180°C, 190°C, and 200°C). The experimental results showed that the dowel bearing strength of MPP degraded at higher temperature and longer exposure durations. MLR and kinetics-based predictive models for dowel bearing strength were also applied in Dillard et al. (2021).

The objective of this study was to characterize the thermal degradation in mechanical properties of MPP nailed connection (including initial stiffness, ultimate strength, and yield strength) through a testing program with eight different temperatures and four exposure times. The yield strength result was compared to the predicted yield strength from NDS formulas (ANSI/AWC 2015) using dowel bearing strength reported by Dillard et al. (2021). In addition, the regression-based and kinetics-based models were utilized to predict the mechanical properties of the nailed connection.

Materials and Methods

MPP was produced from Freres Engineered Wood, Lyons, Oregon. The thickness of these panels was 76.2 mm, and they had a moisture content of approximately 12 percent as received. The MPP consisted of three layers (25.4 mm each layer), which contained nine Douglas-fir veneers per layer. The nailed connection strength and stiffness were investigated as a function of elevated temperature and exposure times. Table 1 presents the experimental plan. There are 33 testing groups, including one control group and 32 exposure groups. Each exposure group is a combination of different elevated temperatures and exposure times. There were six specimens per group, making up a total of 198 specimens in the testing program. A total of eight exposure temperatures (75°C, 100°C, 120°C, 140°C, 160°C, 180°C, 190°C, and 200°C) were evaluated, with four exposure times (0.5, 1.0, 1.5, and 2.0 h) within each temperature (Table 1). A maximum exposure time of 2 hours was chosen to meet the minimum International Building Code specification of a 2-hour fire-resistance rating for structural member (International Code Council 2015).

Nailed connection specimens

The nailed connection consisted of an MPP block (102 by 76 by 152 mm [W by D by H), a 12-gauge galvanized steel plate (25.4 by 178 mm, Grade 33), and an 8d common smooth shank nail (3.4 mm diameter, 63.5 mm long) (Fig. 1). The reason to investigate connections of MPP to steel plates was due to the fact that bracket connections for mass timber panels are now incorporated into the 2021 Special Design Provisions for Wind and Seismic (ANSI/AWC 2021). These brackets are manufactured using 12-gauge American Society for Testing and Materials (ASTM) A653 Grade 33 galvanized steel (ASTM 2009). The bracket is connected to the wall element by eight common nails. Therefore, the performance of these brackets is dependent on the performance of the nails. As a result, our study focused on the performance of a single nailed connection.

A hole was predrilled on the plate for the fastener. The nail was placed 51 mm from the end of the MPP block in the loading direction to avoid any end effect. After the connection specimens were fabricated, they were stored at an ambient temperature of 25°C.

Six specimens in the control group were tested at the ambient temperature of 25°C. The exposure to elevated temperature was conducted in a 6.6-kW drying oven with a volume of 1.15 m^3 and a maximum heating capacity of 200°C. The oven was brought to a temperature slightly above the desired exposure temperature so that by the time specimens were placed and the oven door had closed, the

Table 1.—Experimental plan.

Factor	Quantity	Description
Temperature, °C	8	75, 100, 120, 140, 160, 180, 190, and 200
Time, h	4	0.5, 1.0, 1.5, and 2.0
No. of groups	33	One control group and 32 exposure groups
No. of specimens	6 specimens per group	Total 198 specimens

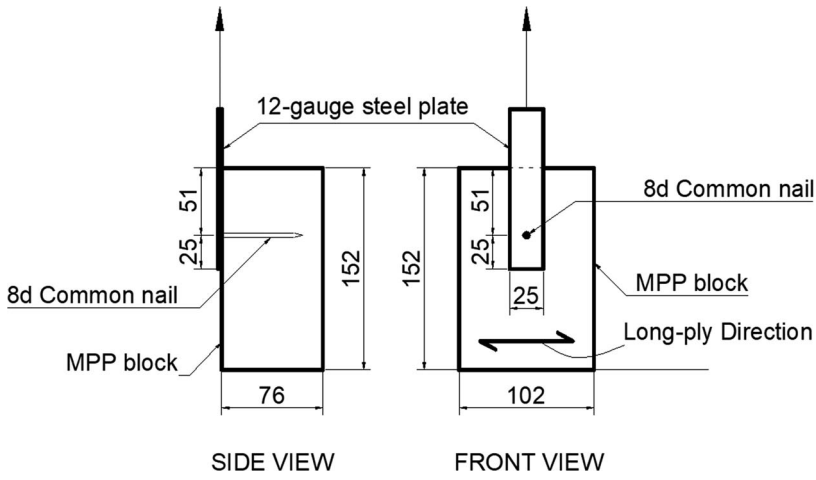

Figure 1.—Nailed connection specimen (dimensions are in millimeters).

oven would be at the desired temperature. Oven temperatures were monitored with an external thermocouple throughout the exposure process and fluctuated within 1°C of the desired temperature. The six specimens would be removed after desired exposure temperature was reached and immediately tested. A separate oven run was conducted for each desired temperature. As discussed by Dillard et al. (2021), the connection strength was affected by the change in moisture and high temperature. However, it is assumed that the slight increase in strength due to reduced moisture content in the specimen was negligible compared to the decrease in strength due to high-temperature exposure.

Test setup

The structural performance of connections under lateral loads was characterized by clamping the MPP block to a steel column and pulling on the steel plate at a constant displacement of 5.0 mm/min using a universal testing machine (Instron 5582; Instron, Norwood, MA) (Fig. 2b). The apparatus was carefully set up to minimize all eccentricities in loading that might cause nail withdrawal. The test direction is perpendicular to the long-ply direction (major strength direction) of MPP panel, which simulated the relative movement between the MPP wall and the bracket under the effect of lateral loads. The crosshead displacement and load were recorded and used to create a load-deflection curve for each specimen. The test was stopped after the load-deflection curve leveled off or the load decreased more than 20 percent from the peak load. Figure 3 shows a typical load-deflection curve for the lateral test of the nailed connection.

Subsequently, the yield load of the connection was determined by applying a 5 percent diameter offset method to the load-deflection curves (ASTM 2007). In this method, the yield load is defined as the intersection of the load deformation (P-Δ) curve and a line parallel to the initial linear portion of the *P-Δ* curve offset positively by 0.05 times the diameter of the nail (Fig. 3). In addition, the slope of the initial linear portion of the *P-Δ* curve and the peak load are defined as the nail connection stiffness and ultimate strength, respectively.

The connection yield strength determined from experiments was compared to the values derived using NDS yield mode equations for dowel-type fasteners without incorporating any reduction factors. The experimental result of dowel bearing strength of MPP reported by Dillard et al. (2021) was utilized in these calculations.

Two different analytical models, including the multiple linear regression (MLR) model and the Arrhenius activation energy model, were developed to predict the mechanical properties of the nailed connection.

MLR model.—The MLR model can help statistically determine relationships between time (t) and temperature (T) effects on the property of interest. The MLR model can be represented under a general form as follows:

$$P = \beta_0 + \beta_1 \times T + \beta_2 \times t + \beta_3 \times Tt \quad (1)$$

where P is the mechanical property of interest, T is an elevated temperature, t is an exposure duration, and β_0 to β_3 are four regression coefficients.

The MLR analysis was performed using all data points instead of mean values for each exposure group. The control specimens were included in the analysis by considering an ambient temperature of 25°C and an exposure time of 0 hours.

Arrhenius activation energy model.—A temperature-dependent degradation rate $k(T)$ was assumed to model each mechanical property as a linear function of exposure duration,

$$P(T,t) = P(T,0) - k(T) \times t \quad (2)$$

where $P(T, 0)$ is the property value at ambient conditions. A straight line was fitted to mean experimental data points at each temperature level T.

First-order kinetics assumes a temperature dependence of the rate constant (Sinha et al. 2011a). We assumed the rate constant $k(T)$ to follow an Arrhenius activation energy equation, given by

$$k(T) = Ae^{-E_a/RT} \quad (3)$$

where A is a constant, E_a is the Arrhenius activation energy, R is the universal gas constant ($R = 8.314$ J K^{-1} mol^{-1}), and T is the absolute temperature (Kelvin).

The fitting can be implemented by applying the logarithmic form of the Arrhenius activation energy equation:

$$\ln\Big(k(T)\Big) = \ln(A) - E_a/RT \quad (4)$$

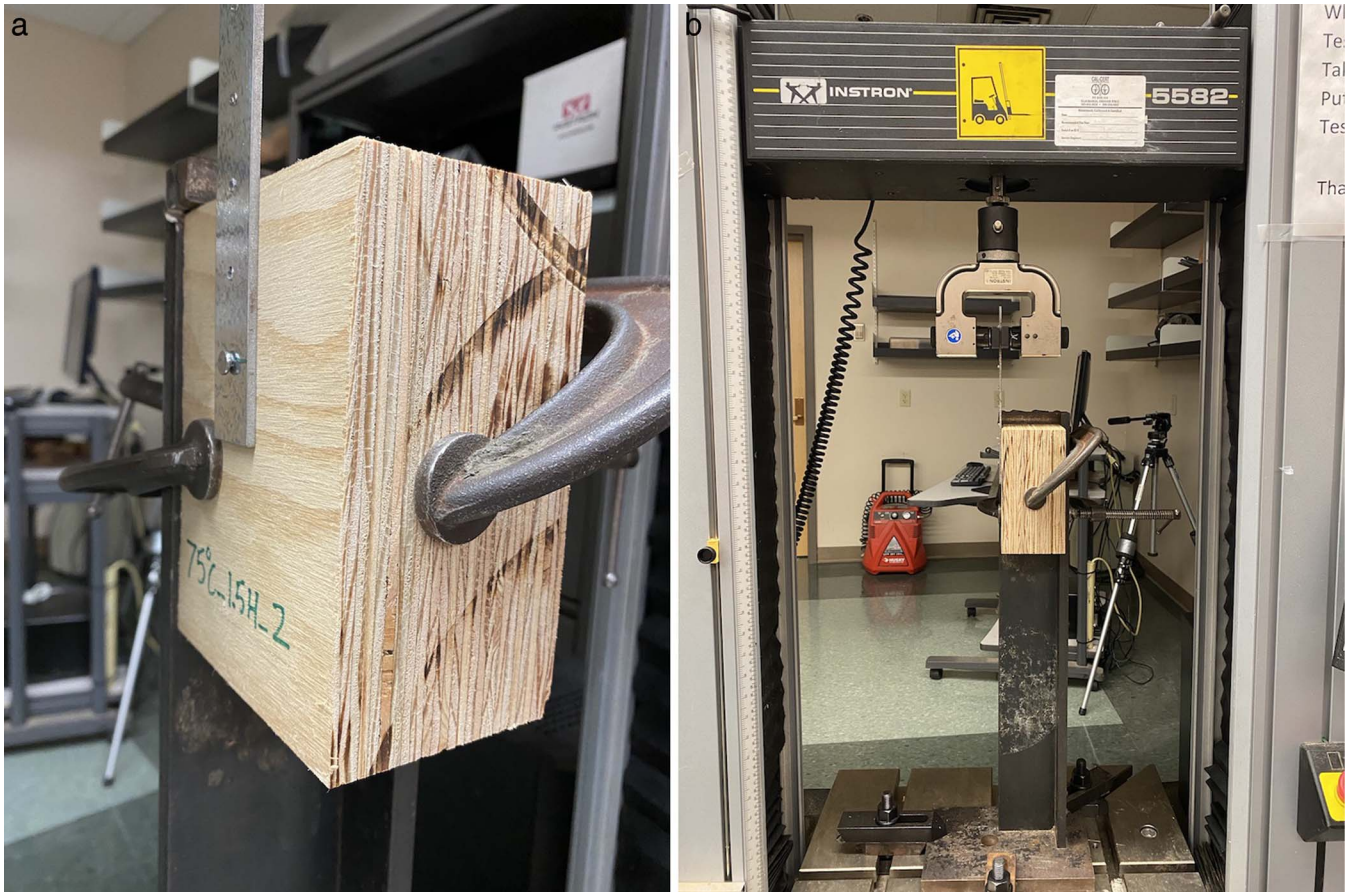

Figure 2.—(a) Details of a specimen and (b) connection test setup.

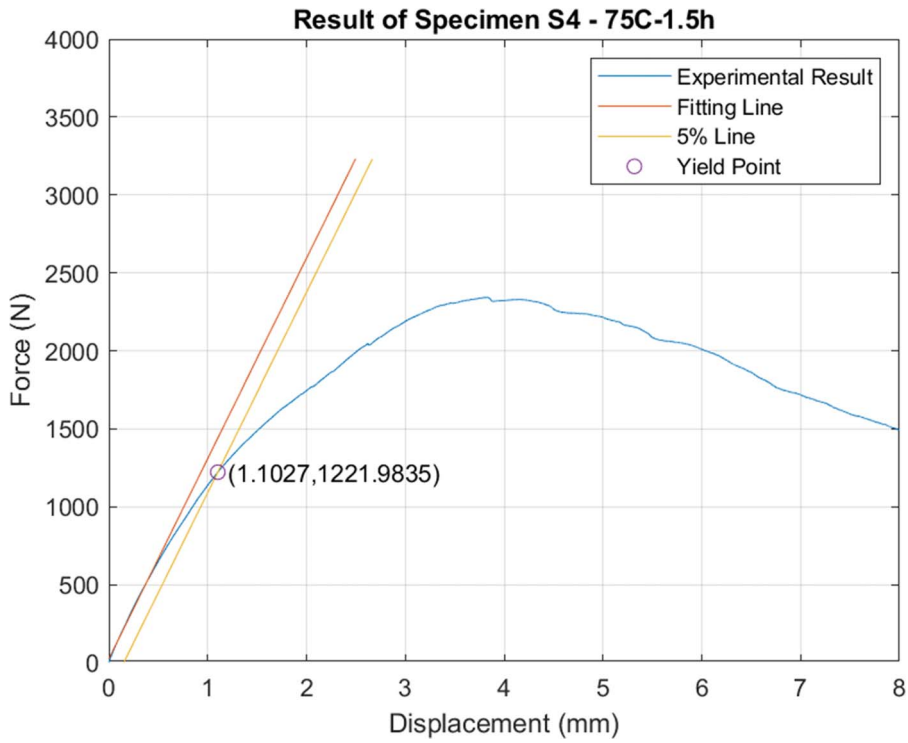

Figure 3.—Typical load deformation (P-Δ) curve of the nail connection and determination of yield load.

Results and Discussion

Testing results

Tables 2 through 4 present the testing results for initial stiffness, ultimate load, and yield load, respectively, of the nail connection corresponding to each combination of exposure temperature and time. It is observed that the initial stiffness and ultimate load at higher temperature and exposure time are lower than those of the control group. The mean initial stiffness of the control group was 1,669 N/mm (coefficient of variation [COV] = 8.9%). Only the specimens in the 75°C/0.5 hour group showed a higher mean stiffness of 1,743 N/mm (COV = 14.4%). However, there is no statistically significant difference between this group and the control group (t test, $P = 0.276$) (Fig. 4a). All statistical comparisons are presented in Figure 4. Twenty-five of 32 exposure groups show a statistically significant reduction in mean initial stiffness compared with the control group. Similarly, mean ultimate load was significantly lower than control group for most of exposure groups except four groups (75°C/0.5 h, 75°C/2.0 h, 100°C/1.0 h, and 120°C/0.5 h) (Fig. 4b). The mean ultimate load for the control group was 2,963 N (COV = 6.9%).

At the same temperature, most groups showed a reduced mean initial stiffness and ultimate load when the exposure duration increased. However, a statistical difference is observed between groups at the same temperature only at 100°C, 140°C, 160°C, and 200°C for initial stiffness (Fig. 4a) and from 100°C to 160°C for ultimate load (Fig. 4b). On the other hand, at the same exposure time, the mean initial stiffness and ultimate load decreased with the increase of temperature. However, the trend could not be statistically confirmed because of high variation. Only groups above 160°C showed statistical difference from groups at 75°C.

In contrast to the trends of initial stiffness and ultimate load, the mean yield load strength showed an increase in 25 of 32 groups compared to the mean value for the control group (Table 4). However, this observed increase was not statistically significant, except for the 160°C/0.5 hour group (Fig. 4c). Specimens exposed to temperatures of 160°C and above showed the highest yield strength in the range of 1,500 to 1,850 N after an exposure time of 0.5 hours, perhaps attributable to the loss of moisture from the specimen.

Failure observations

Three common failure types observed during the tests are shown in Figure 5. The most common failure is a cascading combination of nail pullout, broken nailhead, and wood damage (Fig. 5a), which was reported in 67 percent of total conditioned specimens. The damage in the wood block consisted mainly of crushing around the nail hole, but it manifested in a split in several specimens exposed to higher temperatures (higher than 190°C), as shown in Figure 5b. The second failure type observed was the development of a plastic hinge in the side member (steel plate), breaking at the nail head, but no major damage on the wood block (Fig. 5c), which occurred mainly at temperatures lower than 120°C. This failure mode accounted for 35.6 percent of total specimens tested at this temperature range but only 14.0 percent of all specimens tested. All specimens in the control group also failed in a similar fashion. The last type of failure

Table 2.—Experimental results of the nailed connection test for initial stiffness K_o (N/mm).[a]

	Time and measurements							
	0.5 h		1.0 h		1.5 h		2 h	
Temperature, °C	K_o, MPa	COV, %	K_o, MPa	COV, %	K_o, MPa	COV, %	K_o, MPa	COV, %
75	1,743	14.4	1,563	27.1	1,421	15.3	1,471	16.9
100	1,370	13.1	1,622	18.1	1,205	11.5	1,143	15.6
120	1,457	23.1	1,209	18.4	1,252	10.3	1,188	24.8
140	1,500	9.3	1,105	30.5	1,068	27.3	1,066	14.4
160	1,457	14.2	1,023	16.8	1,100	18.7	1,062	25.5
180	1,100	15.9	1,002	23.2	937	11.1	909	24.5
190	956	13.2	993	18.5	1,043	21.8	1,123	22.5
200	1,281	13.1	1,182	8.7	983	21.7	1,012	9.2

[a] The control group had a $K_o = 1{,}669$ N/mm with a coefficient of variation (COV) of 8.9 percent.

Table 3.—Experimental results of the nailed connection test for ultimate load F_u (N).[a]

	Time and measurements							
	0.5 h		1.0 h		1.5 h		2 h	
Temperature, °C	F_u, N	COV, %	F_u, N	COV, %	F_u, N	COV, %	F_u, N	COV, %
75	2,859	13.1	2,502	0.1	2,589	10.6	2,674	14.8
100	2,620	9.0	2,737	18.9	2,243	11.2	2,164	9.2
120	2,789	9.4	2,282	8.0	2,369	6.8	2,081	9.4
140	2,601	6.6	2,442	8.6	1,982	8.6	1,631	10.9
160	2,683	4.7	2,043	13.5	1,752	7.7	1,689	7.8
180	2,168	9.9	1,862	14.2	1,866	6.0	1,910	12.4
190	2,321	12.3	2,008	9.0	1,904	11.0	2,064	5.2
200	2,104	11.1	1,942	8.3	1,915	12.1	2,083	11.1

[a] The control group had an $F_u = 2{,}963$ N with a coefficient of variation (COV) of 6.9 percent.

Table 4.—Experimental results of the nailed connection test for yield load F_y (N).[a]

	Time and measurements							
	0.5 h		1.0 h		1.5 h		2 h	
Temperature, °C	F_y, N	COV, %	F_y, N	COV, %	F_y, N	COV, %	F_y, N	COV, %
75	1,418	11.0	1,336	0.2	1,356	12.2	1,427	11.1
100	1,292	15.7	1,392	14.3	1,309	31.3	1,241	12.0
120	1,244	20.1	1,526	30.1	1,343	16.6	1,207	18.6
140	1,499	19.0	1,608	31.0	1,331	25.5	1,124	9.8
160	1,835	18.7	1,390	24.6	1,295	8.2	1,197	21.7
180	1,567	36.9	1,299	29.5	1,375	13.1	1,320	23.4
190	1,617	29.4	1,428	19.2	1,218	23.7	1,362	12.5
200	1,542	7.2	1,315	4.4	1,276	17.4	1,319	11.7

[a] The control group had an $F_y = 1{,}281$ N with a coefficient of variation (COV) of 22.2 percent.

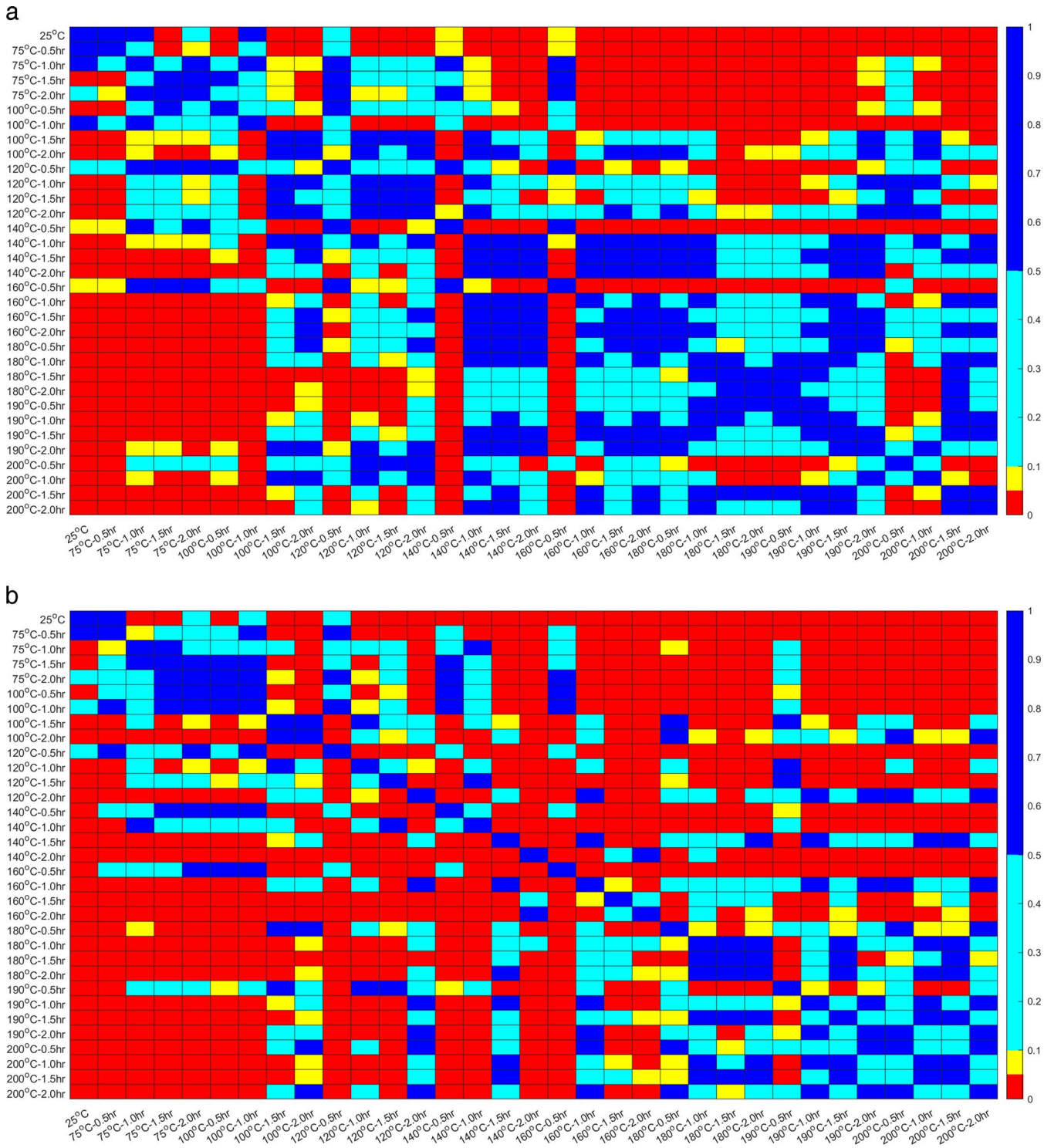

Figure 4.—t-*test results (*P *value) for statistically significant difference between exposure groups: (a) initial stiffness* K_o *(N/mm), (b) ultimate load* F_u *(N), and (c) yield load* F_y *(N).*

was nail pullout and wood crushing (Fig. 5d). This type of failure was observed mainly when the temperature was within 100°C to 160°C and the exposure duration more than 1 hour. This failure mode was seen in only 19 percent of total specimens. The reason of nail pullout as the failure mode at elevated temperatures might be the unequal thermal expansion between wood and steel. During the heat exposure in the drying oven, the steel nail expanded more than the wood block, which would have negligible expansion, resulting in added stress. When the specimen was taken out of the oven, the nail shrunk to its original size. Therefore, a gap, albeit at a microscale, was created between the nail and the wood block and caused a reduction in withdrawal strength of the nail connection.

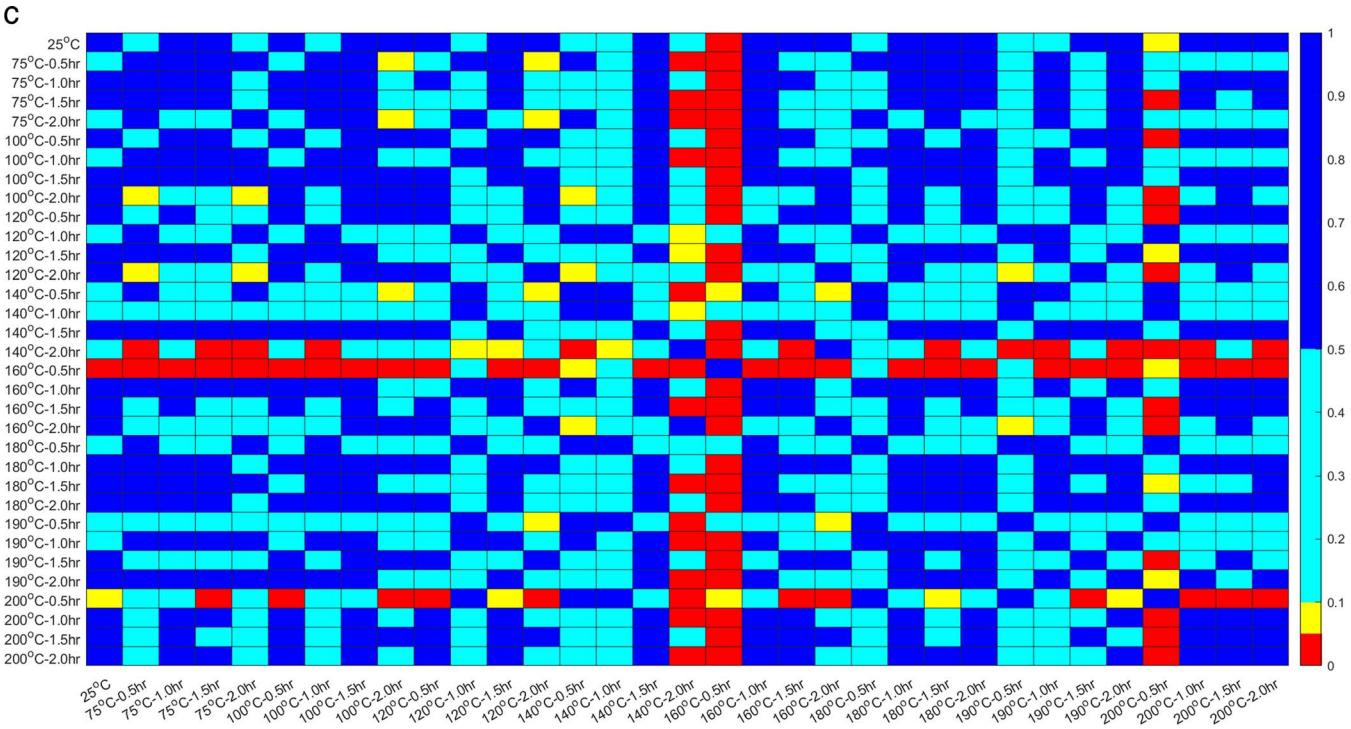

Figure 4.—Continued.

The failure observation suggests that yield mode III_s (ANSI/AWC 2015) dominated at temperatures lower than 120°C. When the temperature exposure increased, the combination of strength degradation in wood and withdrawal strength degradation in the nail connection caused nail pullout. Better contact between the nail and the wood block helps the connection develop higher ultimate strength through the bearing mechanism. However, nail pullout, which occurred at elevated temperatures, prevented the bearing mechanism, and therefore the connection failed at a lower load than at ambient temperature.

Prediction of yield load from experimental dowel bearing strength

Table 5 presents yield load predicted from the results of the dowel bearing test for MPP blocks that were exposed to elevated temperatures (Dillard et al. 2021). Six equations representing different yield modes and a reduction factor of 1.0 were utilized (ANSI/AWC 2015). The predicted yield load was the minimum computed yield mode value of the six possible models. As a result, all the nail connections were predicted to yield at mode III_s, which indicates the formation of the plastic hinge in the fastener and the crushing of the side member (i.e., steel plate). However, during the test, both mode III_s and III_m were observed as discussed above. The predicted value of the control group is 1,268 N, which is very close to the tested mean value of 1,281 N. However, the predicted yield load was reduced with increased temperature and time; this was not captured by the experimental results due to increased variability observed during testing. Increased variability in the observed results rendered any statistical comparison inconclusive. However, 75 percent of the predicted values are within ±1 standard deviation of their corresponding observed values. Another reason of non-convergence between predicted and observed values could be the difference in the dimensions of the samples in this study and the dowel bearing strength test (Dillard et al. 2021). The samples in this study were MPP blocks of 102 by 76 by 152 mm (W by D by H), while the samples in the dowel bearing strength test were MPP blocks of 75 by 75 by 75 mm. Therefore, the thermal effect on specimens in the two studies at the same temperature and exposure time was different, even though the temperature levels, exposure time, heating, and handling techniques were kept consistent between the two studies. As a result of smaller dimensions in the dowel bearing strength test, the yield strength calculated from the test results showed a reduction along with the temperature and exposure time.

Prediction of initial stiffness and ultimate load from analytical models

The analytical models were applied for predicting the initial stiffness and ultimate load of the nail connection but not for yield strength, as there was no statistical evidence of a change of yield strength based on experimental data.

MLR model

The interaction between the exposure time (t) and temperature (T) is assumed and represented by the term $T \times t$ in the full model (i.e., Eq. 1). The regression coefficients were obtained from the MLR analysis. The t test was conducted for each coefficient of the models at a confidence level of 95 percent. The coefficient β_3 in the MLR models for both initial stiffness and ultimate load is

Figure 5.—Failure modes of nail connection specimens: (a) combination of nail pullout, broken nailhead, and wood damage;(b) wood crushing and splitting; (c) broken nailhead without wood damage; and (d) nail pullout and wood crushing.

insignificant ($P > 0.05$), meaning that there is no significant evidence for the interaction between exposure duration and temperature.

Therefore, MLR analysis was implemented for a reduced model of Equation 1 in which the interaction term was not included. The results of the MLR analysis for the reduced model are presented in Table 6. The F values for both models are larger than the minimum F value for significance at the 95 percent confidence level, indicating that the linear regression relationship between the response variable (i.e., initial stiffness and ultimate load) and predictor variables (i.e., exposure time and temperature) is statistically significant. The R^2 result for the reduced models of both initial stiffness and ultimate load is very close to the result of the full models. However, the extra sum-of-squares F test was conducted for the full model and the reduced model, and the result shows a statistically difference between the two models.

Moreover, the R^2 of the MLR models is low, only 0.398 and 0.527 for initial stiffness and ultimate load, respectively, indicating that the MLR model is not good enough for predicting the mechanical properties of MPP nailed connections. Even the interaction term was rendered insignificant. However, it is intuitive that more time at elevated temperature will further reduce properties. As a result, an interaction term is imperative when studying time-dependent thermal effects. Another avenue to consider is the nonlinear representation of data, which might better capture time-dependent thermal effects.

Kinetics-based model using Arrhenius activation energy.—Figure 6 shows the experimental data points of mean initial stiffness and ultimate load as a function of time for each exposure temperature. The regression lines for corresponding temperatures were also plotted. The regression rates $k(T)$, which are the slopes of these regression lines, are presented in Table 7. The degradation rate $k(T)$ increases with temperature and reaches a peak at 180°C and 160°C for initial stiffness and ultimate load, respectively. After that, the degradation rate slightly decreases (~15%) and plateaus. This observation was relatively similar to the observation in cross-laminated timber bracket study conducted by Mahr et al. (2020) in which the degradation rate of ultimate strength peaked at 165°C.

In addition, Table 7 shows that the R^2 values of linear regression for temperatures from 180°C to 200°C are low due to a significant decrease in both initial stiffness and ultimate load of the connection after an exposure duration of 30 minutes (Fig. 6). The change in these mechanical properties after that is not statistically significant.

The linear fittings for degradation rates using the logarithmic form of the Arrhenius activation energy equation are shown in Figure 7 and Table 8. The goodness of linear models (R^2) is 0.820 and 0.798 for degradation rates of initial stiffness and ultimate load, respectively. Moreover, most data points are within 95 percent confident level boundaries. When Equations 2 and 3 were combined to predict the mechanical properties, the kinetics model resulted in good R^2 values of 0.710 and 0.761 for initial stiffness and ultimate load, respectively, especially when compared with the R^2 obtained from the MLR model. The result indicates that the initial stiffness and ultimate load of the nail connection degrade over time at rates that depend on the exposure temperature following the principles of first-order kinetics. This further reinforces that a static model using MLR does not capture all facets of property degradation.

Table 5.—Prediction of yield load: F_y *of control group is 1,268 N.*

	Time and measurements			
Temperature, °C	0.5 h	1.0 h	1.5 h	2 h
75	1,239	1,244	1,226	1,269
100	1,188	1,198	1,138	1,116
120	1,232	1,231	1,211	1,143
140	1,254	1,226	1,234	1,242
160	1,186	1,180	1,175	1,185
180	1,282	1,234	1,167	1,201
190°C	1,269	1,204	1,185	1,155
200°C	1,252	1,253	1,186	1,072

Table 7.—Linear regression result for initial stiffness and ultimate load of the nail connection.

	Stiffness (K_o), N/mm		Ultimate load (F_u), N	
Temperature (T), °C	R^2	$k(T)$	R^2	$k(T)$
75	0.666	111.8	0.430	220.5
100	0.650	259.2	0.858	410.2
120	0.742	287.2	0.884	456.4
140	0.817	367.5	0.983	645.2
160	0.711	376.2	0.930	723.4
180	0.535	476.1	0.453	700.0
190	0.175	408.5	0.511	621.7
200	0.768	403.3	0.199	637.7

Table 8.—Arrhenius activation energy model results.

Parameter	Stiffness (K_o)	Ultimate load (F_u)
A	12,957.0	12,932.2
E_a	12,836.9	11,072.5
R^2	0.820	0.798

Table 6.—Reduced MLR model for nail connection without the interaction term.

	Initial stiffness, N/mm			Ultimate load, N		
Statistic	β_0	β_1	β_2	β_0	β_1	β_2
Value	1,885.8	−3.4793	−142.86	3,282.6	−4.8526	−293.78
P value	6.0×10^{-77}	2.5×10^{-17}	2.0×10^{-6}	2.4×10^{-103}	3.0×10^{-21}	2.1×10^{-14}
Significance	Yes	Yes	Yes	Yes	Yes	Yes
R^2		0.3985			0.5264	
F value		64.59			108.36	

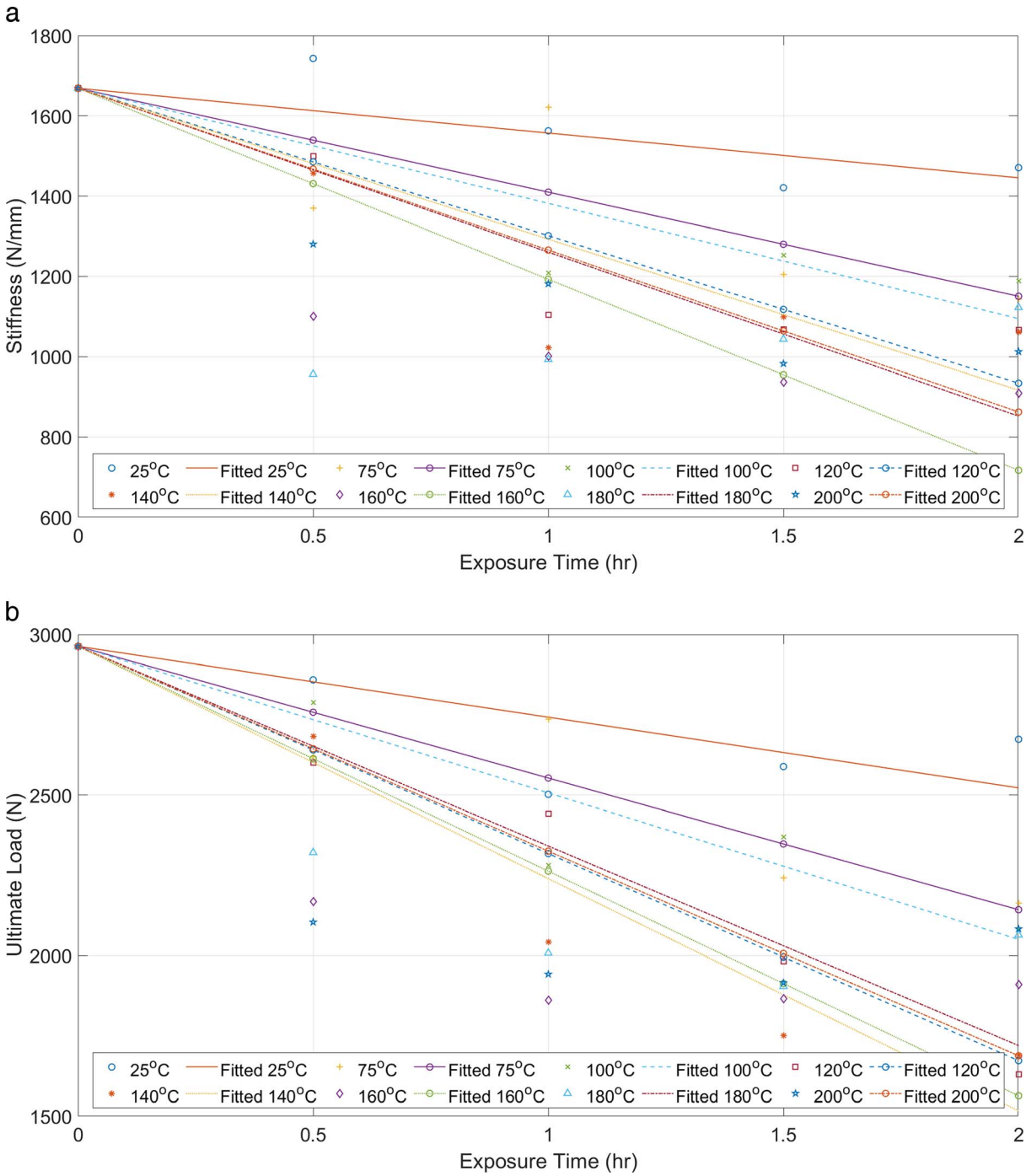

Figure 6.—Fitting of mechanical properties as a linear function of exposure duration: (a) initial stiffness and (b) ultimate load.

Conclusions

The mechanical properties of MPP nail connection under the effects of eight different temperatures and four exposure durations were experimentally investigated. Three common failure types were observed in tested samples, including nail pullout, broken nailhead, and wood damage. The failure observation suggests failure mode III_s at temperatures lower than 120°C and mode III_m at higher temperatures.

The test results show that initial stiffness and ultimate load of the connection samples were reduced under the effect of thermal exposure, compared to the control samples, up to 45 percent. The mean values of these properties also decreased with the increase of exposure temperature and time, but the decrease was not statistically significant at the 95 percent confidence level. Two predictive models were studied: one based on MLR and one on first-order kinetics. The interaction between temperature and exposure time was not significant in the full MLR models for initial stiffness and ultimate load. Therefore, the interaction term was removed in the reduced MLR model. The kinetics-based model suggested a time- and temperature-dependent degradation rate. Additionally, a substantially better correlation was observed than in the MLR. Therefore, the Arrhenius

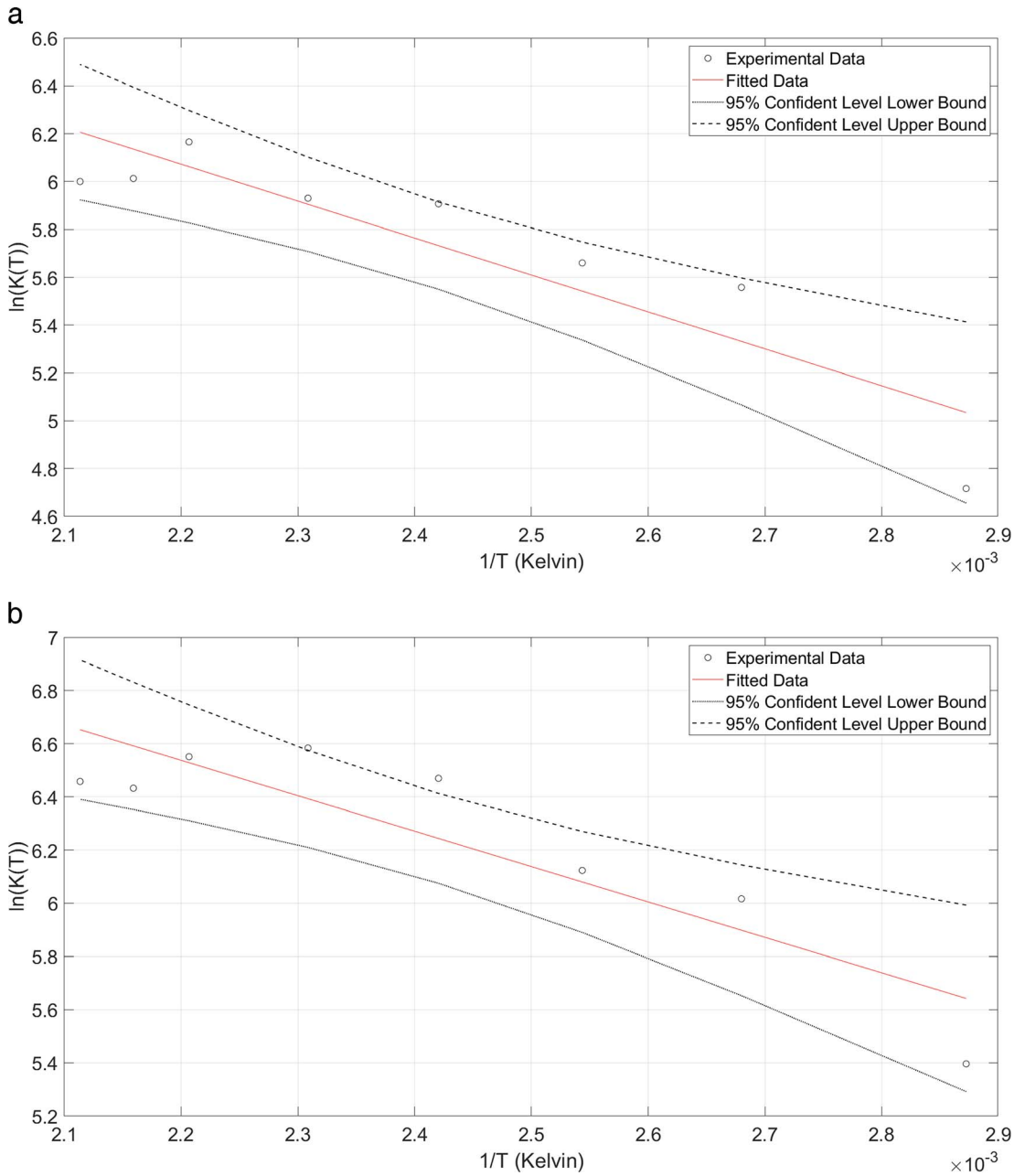

Figure 7.—Fitting of rate of degradation in the logarithmic form of the Arrhenius activation energy for (a) stiffness and (b) ultimate load.

activation energy model is preferred, as it provided better predictions than the MLR model. The result indicates that the initial stiffness and ultimate load of the nail connection degrade over time at rates depending on the exposure temperature.

On the other hand, the experimental results show no statistical evidence for the change of yield load in the majority of testing groups, which is opposite to the prediction from the NDS formulas and the dowel bearing strength test result (Dillard et al. 2021). This can be explained by the differences in sample dimensions between the two studies and in the failure modes between the experiment and the NDS prediction. Therefore, further studies are needed to quantify the effect on yield strength using complementary dowel bearing strength data.

Acknowledgment

We extend our acknowledgment to the US Department of Agriculture (USDA) for providing funding for the second author to work on the project through AFRI ELI grant no. 2021- 67037-34623 from the USDA National Institute of Food and Agriculture.

Literature Cited

Akgul, T. and A. Sinha. 2016. Degradation of yield strength of laterally loaded wood-to-oriented strandboard connections after exposure to elevated temperatures. *Wood Fiber Sci*. 48(2):59–67.

American National Standards Institute/American Wood Council (ANSI/AWC). 2015. National Design Specification for Wood Construction. ANSI/AWC, Washington, DC.

American National Standards Institute/American Wood Council (ANSI/

AWC) (2021). Special Design Provisions for Wind and Seismic. ANSI/AWC, Washington, DC.
American Society for Testing and Materials (ASTM). 2007. Standard test method for determining bending yield moment of nails. ASTM D1761. ASTM, West Conshohocken, Pennsylvania.
American Society for Testing and Materials (ASTM). 2009. Standard specification for steel sheet, zinc-coated (galvanized) or zinc-iron alloy-coated (galvannealed) by the hot-dip process. ASTM A653. ASTM, West Conshohocken, Pennsylvania.
Dillard, A., T. X. Ho, A. Indra, and A. Sinha. 2021. Effect of exposure to elevated temperature on dowel bearing strength of mass plywood panels. *Wood Fiber Sci*. 53(4):273–280.
Fuller, J. J. 1990. Predicting the thermo-mechanical behavior of a gypsum-to-wood nailed connection. Master's thesis, Oregon State University, Corvallis.
Ho, X. T., A. Arora, and A. Sinha. 2022. In-plane shear properties of mass ply panels in long-ply direction. *J. Mater. Civil Eng*. 34(8). https://ascelibrary.org/doi/full/10.1061/%28ASCE%29MT.1943-5533.0004327
International Code Council. 2015. International Building Code. International Code Council, Country Club Hills, Illinois.
Mahr, K., A. Sinha, and A. R. Barbosa. 2020. Experimental investigation and modeling of thermal effects on a typical cross-laminated timber bracket shear connection. *J Mater. Civil Eng*. 32(6).doi:10.1061/(ASCE)MT.1943-5533.0003122
Miyamoto, B. T., A. Sinha, and I. Morrell. 2020. Connection performance of mass plywood panels. *Forest Prod. J*. 70(1):88–99. https://doi.org/10.13073/FPJ-D-19-00056
Morrell, I., R. Soti, B. Miyamoto, and A. Sinha. 2020. Experimental investigation of base conditions affecting seismic performance of mass plywood panel shear walls. *J. Struct. Eng*. 146(8). doi:10.1061/(asce)st.1943-541x.0002674
Noren, J. 1996. Load-bearing capacity of nailed joints exposed to fire. *Fire Mater*. 20:133–143.
Peyer, S. M. and S. M. Cramer. 1999. Behavior of nailed connections at elevated temperatures. *Wood Fiber Sci*. 31:264–276.
Shrestha, D., S. M. Cramer, and R. White. 1995. Simplified models for the properties of dimension lumber and metal-plate connections at elevated temperatures. *Forest Prod. J*. 45(7/8):35–42.
Sinha, A. 2013. Thermal degradation modeling of flexural strength of wood after exposure to elevated temperatures. *Wood Mater. Sci. Eng*. 8:111–118.
Sinha, A., R. Gupta, and J. A. Nairn. 2011a. Thermal degradation of bending properties of structural wood and wood-based composites. *Holzforschung* 65:221–229. https://doi.org/10.1515/HF.2011.001
Sinha, A., R. Gupta, and J. A. Nairn. 2011b. Thermal degradation of lateral yield strength of nailed wood connections. *J. Mater. Civil Eng*. 23:812–822. doi:10.1061/(ASCE)MT.1943-5533.0000233
Sinha, A., I. Morrell, and T. Akgul. 2018. Thermal degradation modeling for single-shear nailed connections. *Wood Mater. Sci. Eng*. 13:16–20. doi:10.1080/17480272.2016.1226947
Sinha, A., J. A. Nairn, and R. Gupta. 2011c. Thermal degradation of bending strength of plywood and oriented strand board: A kinetics approach. *Wood Sci. Technol*. 45:315–330. doi:10.1007/s00226-010-0329-3
Sinha, A., J. A. Nairn, and R. Gupta. 2012. The effect of elevated temperature exposure on the fracture toughness of solid wood and structural wood composites. *Wood Sci. Technol*. 46:1127–1149.
Soti, R., T. X. Ho, and A. Sinha. 2021. Structural performance characterization of mass plywood panels. *J. Mater. Civil Eng*. 33(10):04021275.
Soti, R., A. Sinha, I. Morrell, and B. T. Miyamoto. 2020. Response of self-centering mass plywood panel shear walls. *Wood Fiber Sci*. 52:102–116. https://doi.org/10.22382/wfs-2020-009